Article:

Jenkin, M. E., Khan, M. A. H., Shallcross, D. E. et al. (4 more authors) (2019) The CRI v2.2 reduced degradation scheme for isoprene. Atmospheric Environment. pp. 172-182. ISSN 1352-2310

https://doi.org/10.1016/j.atmosenv.2019.05.055

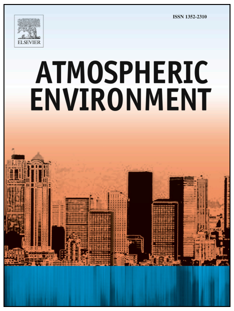

The CRI v2.2 reduced degradation scheme for isoprene

M.E. Jenkin, M.A.H. Khan, D.E. Shallcross, R. Bergström, D. Simpson, K.L.C. Murphy, A.R. Rickard

PII: S1352-2310(19)30360-7

DOI: https://doi.org/10.1016/j.atmosenv.2019.05.055

Reference: AEA 16747

To appear in: *Atmospheric Environment*

Received Date: 22 March 2019

Revised Date: 20 May 2019

Accepted Date: 23 May 2019

Please cite this article as: Jenkin, M.E., Khan, M.A.H., Shallcross, D.E., Bergström, R., Simpson, D., Murphy, K.L.C., Rickard, A.R., The CRI v2.2 reduced degradation scheme for isoprene, *Atmospheric Environment* (2019), doi: https://doi.org/10.1016/j.atmosenv.2019.05.055.

The CRI v2.2 reduced degradation scheme for isoprene

M. E. Jenkin [1,2,*], M. A. H. Khan [2], D. E. Shallcross [2], R. Bergström [3,4], D. Simpson [5,3], K. L. C. Murphy [6,7] and A. R. Rickard [6,7]

[1] Atmospheric Chemistry Services, Okehampton, Devon, EX20 4QB, UK;

[2] School of Chemistry, University of Bristol, Cantock's Close, Bristol, BS8 1TS, UK;

[3] Department of Space, Earth and Environment, Chalmers University of Technology, 41296 Gothenburg, Sweden;

[4] Swedish Meteorological and Hydrological Institute, 601 76 Norrköping, Sweden

[5] EMEP MSC-W, Norwegian Meteorological Institute, Oslo, 0313 Oslo 3, Norway;

[6] Wolfson Atmospheric Chemistry Laboratories, Department of Chemistry, University of York, York, YO10 5DD, UK.

[7] National Centre for Atmospheric Science, University of York, York, YO10 5DD, UK.

* Corresponding author. E-mail address: atmos.chem@btinternet.com (M. E. Jenkin)

Abstract

The reduced representation of isoprene degradation in the Common Representative Intermediates (CRI) mechanism has been systematically updated, using the Master Chemical Mechanism (MCM v3.3.1) as a reference benchmark, with the updated mechanism being released as CRI v2.2. The complete isoprene degradation mechanism in CRI v2.2 consists of 186 reactions of 56 closed shell and free radical species, this being an order of magnitude reduction in size compared with MCM v3.3.1. The chemistry initiated by reaction with OH radicals, NO_3 radicals and ozone (O_3) is treated. An overview of the updates is provided, within the context of reported kinetic and mechanistic information. The revisions mainly relate to the OH-initiated chemistry, which tends to dominate under atmospheric conditions, although these include updates to the chemistry of products that are also generated from the O_3- and NO_3-initiated oxidation. The revisions have impacts in a number of key areas, including recycling of HO_x and NO_x. The performance of the CRI v2.2 isoprene mechanism has been compared with those of the preceding version (CRI v2.1) and the reference MCM v3.3.1 over a range of relevant conditions, using a box model of the tropical forested boundary layer. In addition, tests are carried out to ensure that the performance of MCM v3.3.1 remains robust to more recently reported information. CRI v2.2 has also been implemented into the STOCHEM chemistry-transport model, with a customized close-variant of CRI v2.2 implemented into the EMEP MSC-W chemistry-transport model. The results of these studies are presented and used to illustrate the global-scale impacts of the mechanistic updates on HO_x radical concentrations.

Keywords: Tropospheric chemistry; Biogenic hydrocarbons; Degradation mechanisms; HO_x recycling; Mechanism reduction.

1 Introduction

The degradation of emitted volatile organic compounds (VOCs) has a major influence on the chemistry of the troposphere, contributing to the formation of ozone (O_3), secondary organic aerosol (SOA) and other secondary pollutants (e.g. Haagen-Smit and Fox, 1954; Went, 1960; Andreae and Crutzen, 1997; Jenkin and Clemitshaw, 2000; Hallquist et al., 2009). Biogenic sources are reported to dominate emissions of organic material on a global scale (Guenther et al., 2012), with the reactive biogenic VOC isoprene (2-methyl-buta-1,3-diene) making a major contribution. On a regional scale over Europe, isoprene is estimated to contribute more than 30 % of total biogenic VOC emissions, and 50 % of reactive biogenic VOC emissions (Simpson et al., 1999). Although there is a wide variation in both regional and global estimates (e.g. Arneth et al. 2008, Warneke et al., 2010, Langner et al., 2014), isoprene is believed to be the most abundantly emitted non-methane VOC in the atmosphere. Its emission rate may also be altered by future changes to climate and other environmental factors (e.g. Peñuelas and Staudt, 2010, Arneth et al, 2010, Simpson et al., 2014, and references therein). Reliable representations of the emissions and atmospheric oxidation chemistry of isoprene are therefore important components of chemistry-transport models (CTMs) applied to climate change and air quality assessments.

There have been some notable advances in the understanding of atmospheric isoprene chemistry over the past decade (e.g. Wennberg et al., 2018; and references therein), particularly in relation to recycling mechanisms for HO_x radicals (i.e. OH and HO_2), the chemistry of oxidized organic nitrogen species and the formation of species that contribute to SOA. This has been reflected in recent updates to detailed explicit gas-phase mechanisms, such as version 3.3.1 of the Master Chemical Mechanism, MCM v3.3.1 (Jenkin et al., 2015), which includes 1926 reactions of 602 species describing the complete gas phase oxidation of isoprene. Although such a mechanism cannot be used directly in applications requiring great computational efficiency, it provides a traceable link to elementary kinetic and mechanistic studies, and a reference benchmark mechanism against which to develop, evaluate and optimize reduced chemical mechanisms. MCM v3.3.1 is thus used as the reference mechanism in the present work. Given its importance, new information on atmospheric isoprene chemistry is constantly emerging, and there have inevitably been some further advances since the release of MCM v3.3.1 in 2015. These have been reviewed recently by Wennberg et al. (2018), with a nearly complete gas-phase oxidation mechanism of isoprene and its major products also reported. As part of the present study, the impacts of some of the main mechanistic differences compared with MCM v3.3.1 have been examined for a range of relevant conditions, using a box model of the tropical forested boundary layer. The results of these comparisons are presented and discussed in Sect. 4 and in the Supplement (Sect. S2).

The Common Representative Intermediates (CRI v2) mechanism is a reduced (lumped chemistry) scheme of intermediate complexity (Jenkin et al., 2008). It was built up on a compound-by-compound basis for 115 non-methane VOCs, with the O_3-forming ability of its chemistry optimised for each compound in turn by comparison with that of an earlier version of the Master Chemical Mechanism (MCM v3.1), using box model simulations (Jenkin et al., 2008). A key assumption in the construction method is that the potential for O_3 formation from a given VOC is related to the number of reactive (i.e. C-C and C-H) bonds it contains. This index allows generic intermediates to be defined, with each being used to represent a set of species possessing the same index, as formed in detailed mechanisms such as the MCM. A series of five progressively more reduced variants (CRI v2-R1 to CRI v2-R5) was also subsequently developed, using systematic and tested lumping of anthropogenic VOC emissions (Watson et al., 2008). The smallest of these (CRI v2-R5) has 609 reactions of 220 species, with the suite of emitted non-methane VOCs represented by 22 compounds. However, all these reduced v2 variants contain the same isoprene chemistry as CRI v2, consisting of 113 reactions of 43 species. Although still quite detailed, CRI v2-R5 has routinely been used in the 3-D global CTM, STOCHEM-CRI (e.g. Utembe et al., 2010; Khan et al., 2017), and both CRI v2 and CRI v2-R5 are among several mechanisms available to the 3-D European regional and global CTM, EMEP MSC-W (Simpson et al., 2012, 2018; McFiggans et al. 2019).

The CRI isoprene chemistry has been systematically revised and updated to reflect the recent advances in understanding (as represented in MCM v3.3.1), with the revised chemistry being released as part of CRI v2.2. These updates are described in Sect. 3. The performance of the CRI v2.2 isoprene scheme has been examined for a range of relevant conditions, using the tropical forested boundary layer box model, and is compared with those of MCM v3.3.1 and the immediately preceding CRI v2.1[1] in Sect. 4. In addition, CRI v2.2 has been implemented into the STOCHEM-CRI model, with a customized close-variant of CRI v2.2 implemented into the EMEP MSC-W model. The results of these studies are presented and used to illustrate the global-scale impacts of the mechanistic updates on HO_x radical concentrations.

2 Model description

2.1 Zero-dimensional boundary layer box model

The impact of recent mechanistic advances compared with MCM v3.3.1, and the performance of the CRI v2.2 isoprene mechanism, were examined in detail using simulations carried out with the box model of the tropical forested boundary layer applied previously by Jenkin et al. (2015), coded for application with the FACSIMILE kinetics integration package (MCPA Software). The aim of these studies was to test and compare the performance of the mechanisms for a range of idealised atmospheric conditions, with particular emphasis on the impacts of mechanistic differences on the partitioning and recycling of HO_x and NO_x.

The model was designed to simulate a well-mixed tropical forested boundary layer, 1000 m in depth. The boundary layer air parcel was continuously exchanged with the free troposphere on a timescale of 1 day, thus representing a loss process for longer-lived products. The free troposphere was assumed to contain the following limited series of trace species, which were mixed into the boundary layer on the same timescale: O_3 (20 ppb), CO (100 ppb), and HCHO (300 ppt). The model

---

[1] Prior to the present work, the prevailing version of the mechanism was CRI v2.1. This contained the same reaction set as CRI v2, but with some generic rate coefficient revisions in parallel with those in the MCM v3.1 to v3.2 transition. The performance of the isoprene chemistry in v2 and v2.1 is therefore almost identical.

was initialised for seven days such that exchange processes reached steady state, and results from the daylight portion of the eighth diurnal cycle were used in comparisons of mechanism performance. The temperature followed a sinusoidal diurnal profile (average 298 K; amplitude 4 K), leading to a peak temperature of 302 K in the early afternoon.

The diurnal variation of photolysis parameters was set for latitude 0° at equinox in all simulations. Photolysis coefficients were calculated assuming clear sky conditions, using a parameterization previously applied with the MCM (Saunders et al., 2003). For the present illustration, the loss of product species via deposition or transfer to the condensed phase was not represented, the focus of the simulations being chemical processing in the gas phase. The same inorganic reaction scheme and parameters were used with each mechanism, so that the differences in performance result from the differences in the organic chemistry, as summarised in Table 1.

Table 1. Isoprene mechanisms and mechanistic variants considered in the present work.

Mechanism	Description	Comment
MCM v3.3.1	Reference mechanism (Jenkin et al., 2015). Available at: http://mcm.york.ac.uk/.	-
CAL 1	MCM v3.3.1 with OH attack distribution, rate coefficients for reversible addition of O_2 to OH-isoprene adducts and for 1,6 H-shift reactions of *Z*-δ-hydroxy peroxy isomers based on Wennberg et al. (2018).	(a)
CAL 2	CAL 1 with products of 1,6 H-shift reactions of *Z*-δ-hydroxy peroxy isomers and of first-generation β-hydroxy peroxy isomer + HO_2 reactions based on Wennberg et al. (2018).	(b)
CAL 3	CAL 2 with fates of first-generation oxy radicals based on Wennberg et al. (2018).	(c)
CAL 4	CAL 3 with product ratios for first-generation RO_2 + NO reactions based on Wennberg et al. (2018).	(d)
CRI v2.2	Reduced mechanism. Available at: http://cri.york.ac.uk/.	-
CRI v2, v2.1	Preceding versions of the reduced mechanism.	(e)

Comments

[a] The *Z*-δ-hydroxy peroxy isomers are denoted CISOPAO2 and CISOPCO2 in MCM v3.3.1 and *Z*-δ-1,4-ISOPOO and *Z*-δ-4,1-ISOPOO by Wennberg et al. (2018); [b] Wennberg et al. (2018) recommend partial formation of β-hydroperoxy-aldehydes from 1,6 H-shift reactions. These species and their degradation chemistry were added to the mechanism according to Wennberg et al. (2018). Minor propagating channels included for reactions of HO_2 with β-hydroxy peroxy radicals, denoted ISOPBO2 and ISOPDO2 in MCM v3.3.1 and β-1,2-ISOPOO and β-4,3-ISOPOO by Wennberg et al. (2018); [c] Adjusted fates incorporated for *Z*-δ-hydroxy oxy radicals, denoted CISOPAO and CISOPCO in MCM v3.3.1 and *Z*-δ-1,4-ISOPO and *Z*-δ-4,1-ISOPO by Wennberg et al. (2018); [d] The weighted average branching ratios for nitrate formation from first-generation RO_2 + NO reactions recommended by Wennberg et al. (2018) is about 33 % higher than that applied in MCM v3.3.1 at 298 K and 760 Torr; [e] These earlier versions (including the subset mechanism CRI v2-R5) contain identical sets of reactions describing isoprene degradation. CRI v2.1 is also available for download in FACSIMILE and KPP formats at http://cri.york.ac.uk/download.htt.

The boundary layer box received continuous emissions of isoprene and NO_x, which were maintained throughout the model runs, and a fixed mixing ratio of 1.8 ppm methane was assumed. A constant base NO_x emission rate of 4.7×10^9 molecule cm^{-2} s^{-1} was applied, which is a globally averaged rate based on an annual total emission of 44.8 TgN, as applied by Derwent et al. (2003). This resulted in a daylight-averaged NO_x mixing ratio of about 34 ppt in the MCM v3.3.1 simulation. To examine the NO_x dependence of the chemistry, the NO_x emission rate was scaled by factors of 3, 10, 30, 100 and 200 which resulted in daylight-averaged NO_x mixing ratios up to about 8 ppb.

The relative isoprene emission rate varied with temperature and photosynthetically active radiation (PAR) throughout the diurnal cycle, based on a standard algorithm (Guenther et al., 1995). The absolute magnitude of the emissions was set such that the daylight average emission rate was 7.6×10^{11} molecule cm^{-2} s^{-1} (3.1 μgm^{-2} h^{-1}), maximising at 1.0×10^{12} molecule cm^{-2} s^{-1} (4.2 μgm^{-2} h^{-1}) in the early afternoon. These emissions fluxes are typical of those reported for tropical forested regions (e.g. Eerdekens et al., 2009).

Reaction with OH was the dominant fate of isoprene for the conditions of this illustration, accounting for between 89 and 93 % of isoprene removal in the MCM v3.3.1 simulations (depending on the NO_x level). The contribution of the O_3-initiated chemistry increases from about 4 % at the high end of the NO_x range to about 11 % at the low end of the NO_x range. The NO_3-initiated chemistry is also simulated to contribute up to about 4 % to isoprene removal, with the maximum contribution towards the high end of the NO_x range.

2.2 3-D global modelling

The impacts of the mechanistic updates on global scale HO_x radical concentrations have been examined using the well-documented 3-D global CTMs, STOCHEM-CRI (Utembe et al., 2010; Khan et al., 2017), and EMEP MSC-W (Simpson et al., 2012, 2018; Stadtler et al., 2017, McFiggans et al. 2019), which have been described in detail elsewhere. The implementation of CRI v2-R5 into the STOCHEM model has been reported previously by Utembe et al. (2010). In the present study, the impacts of updating the isoprene chemistry to CRI v2.2 are presented. In the case of the EMEP MSC-W model, a closely-related bespoke version of the CRI v2.2 chemistry is applied, which performs consistently in relation to all the main criteria considered here (see Sects. 3.1 and S1 for further details). The performance of the isoprene mechanism relative to that of CRI v2.1 is illustrated.

The emissions of biogenic VOCs differ slightly between the models. EMEP MSC-W applies isoprene emissions of 425 Tg/yr, and monoterpene emissions of 129 Tg/yr, all from terrestrial sources (Simpson et al., 2018). STOCHEM-CRI applies terrestrial isoprene emissions of 501 Tg/yr and monoterpene emissions of 127 Tg/yr (Utembe et al., 2010), with oceanic isoprene emissions of 1.9 Tg/yr also recently included, based on Arnold et al. (2009). Although based upon entirely different land-cover maps and methodologies, the differences in the terrestrial isoprene and terpene emissions are therefore small compared to the range of values found in the literature (e.g. Arneth et al., 2008).

3 Updates to isoprene chemistry in CRI v2.2

The complete degradation chemistry of isoprene, as represented in CRI v2.2, consists of 186 reactions of 56 species and includes chemistry initiated by reaction with OH, O_3 and NO_3. It can be accessed via the new MCM website at the University of York (http://mcm.york.ac.uk/) or directly at http://cri.york.ac.uk/, where the mechanism can be viewed and downloaded using the subset mechanism assembling facility. As described previously by Jenkin et al. (2008) and Archibald et al. (2010a; 2010b), the isoprene chemistry included previously in CRI v2 and CRI v2.1 was developed and optimized so that its performance matched that of MCM v3.1. The updates described below therefore document the major changes to the mechanism since CRI v2.1. The revisions mainly relate to the OH-initiated chemistry, which tends to dominate under atmospheric conditions, although these include updates to the chemistry of some products that are also generated from the O_3- and NO_3-initiated oxidation.

3.1 Updates to the first-generation OH-initiated chemistry

The initial stages of the chemistry following addition of OH in the presence of O_2, as represented in CRI v2.2, are shown in Fig. 1. The reaction forms a single lumped peroxy radical (RU14O2), which is representative of a set of six isomeric peroxy radicals formed following the (major) addition of OH to the two terminal carbon atoms in isoprene. The minor addition to the two central carbon atoms is not represented in CRI v2.2, this only accounting for about 8 % of the reaction in MCM v3.3.1. Similarly to previous CRI versions, RU14O2 undergoes traditional bimolecular reactions with NO, NO_3, HO_2 and the pool of peroxy radicals (RO_2) in CRI v2.2, but with rate coefficients and product ratios revised (where necessary) based on those in MCM v3.3.1.

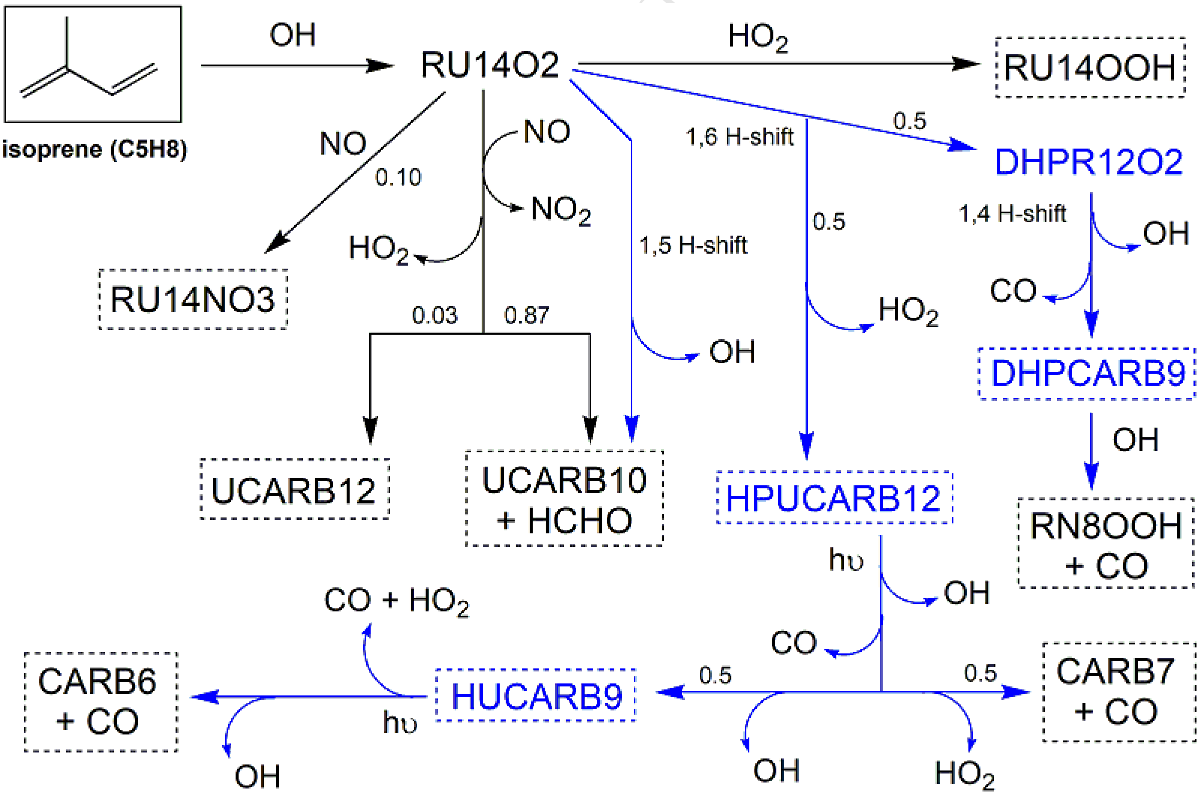

Figure 1: Schematic of the main features of the OH-initiated oxidation of isoprene to first-generation closed-shell products (shown in boxes), as represented in CRI v2.2. The main features of the chemistry following rapid photolysis of HPUCARB12 and HUCARB9, and reaction of DHPCARB with OH, are also shown. Species and routes shown in blue are new in CRI v2.2. For clarity, the scheme omits the reactions of RU14O2 with NO_3 and the peroxy radical pool, and all bimolecular reactions of DHPR12O2, although these are included in the mechanism. Further information on species class and identity is given in Table S3.

The most significant update to the first generation chemistry is the inclusion of 1,5 H-shift and 1,6 H-shift isomerization reactions for RU14O2 (and subsequent chemistry), characterized as part of the Leuven Isoprene Mechanism (LIM1) reaction framework developed by Peeters et al. (2009; 2014), as applied in MCM v3.3.1. As shown in Fig. 1, these provide additional routes that recycle and generate HO_x radicals (i.e. OH and HO_2), which are particularly significant under NO_x-limited conditions. In practice, each type of isomerization is only available for a subset of the peroxy radicals represented by RU14O2, specifically two β-hydroxy isomers for the 1,5 H-shift reaction and two *Z*-δ-hydroxy isomers for the 1,6 H-shift reaction. As discussed previously (e.g. Peeters et al., 2014; Jenkin et al., 2015; Wennberg et al., 2018) the effective rate coefficients assigned to these reactions for a lumped peroxy radical therefore need to take account of the relative population of the component peroxy radical isomers under atmospheric conditions, and the prevailing total removal rate via the competing traditional bimolecular reactions (k_{tr}). These were based on simulations of the effective bulk isomerization rates, using MCM v3.3.1. Because the peroxy radical population is dominated by the β-hydroxy isomers over the typical range of atmospheric conditions, the bulk 1,5 H-shift reaction could be represented acceptably by a single rate coefficient expression based on the weighted average of those applied to the β-hydroxy isomers in MCM v3.3.1 (see Sect. S1.1). However, the effective rate of the (more important) bulk 1,6 H-shift reaction ($k_{bulk\ 1,6\ H}$) varies approximately linearly with k_{tr} over the typical tropospheric range of conditions, as first discussed by Peeters et al. (2014). It is therefore represented by an expression of the following form (k_0 and A are fitted constants):

$$k_{bulk\ 1,6\ H} = k_0 + (k_{tr} \times A) \qquad \text{(i)}$$

This is discussed further in Sect. S1.1. However, to provide an alternative to the use of the conditions-dependent rate coefficient in Eq. (i), a more explicit reduced representation of the chemistry was also developed, using a set of three isomeric peroxy radicals to represent the six formed in MCM v3.3.1. This alternative representation was applied in the EMEP MSC-W model, and is described in more detail in Sect. S1.1.

Analogously to MCM v3.3.1, two product channels are represented for the 1,6 H-shift reaction (see Fig. 1), leading either to the formation of HO_2 and a lumped unsaturated δ-hydroperoxyaldehyde product (HPUCARB12) or a lumped dihydroperoxy formyl peroxy radical (DHPR12O2), which reacts significantly via a 1,4 H-shift isomerization reaction to form OH, CO and a dihydroperoxy carbonyl product (DHPCARB9).

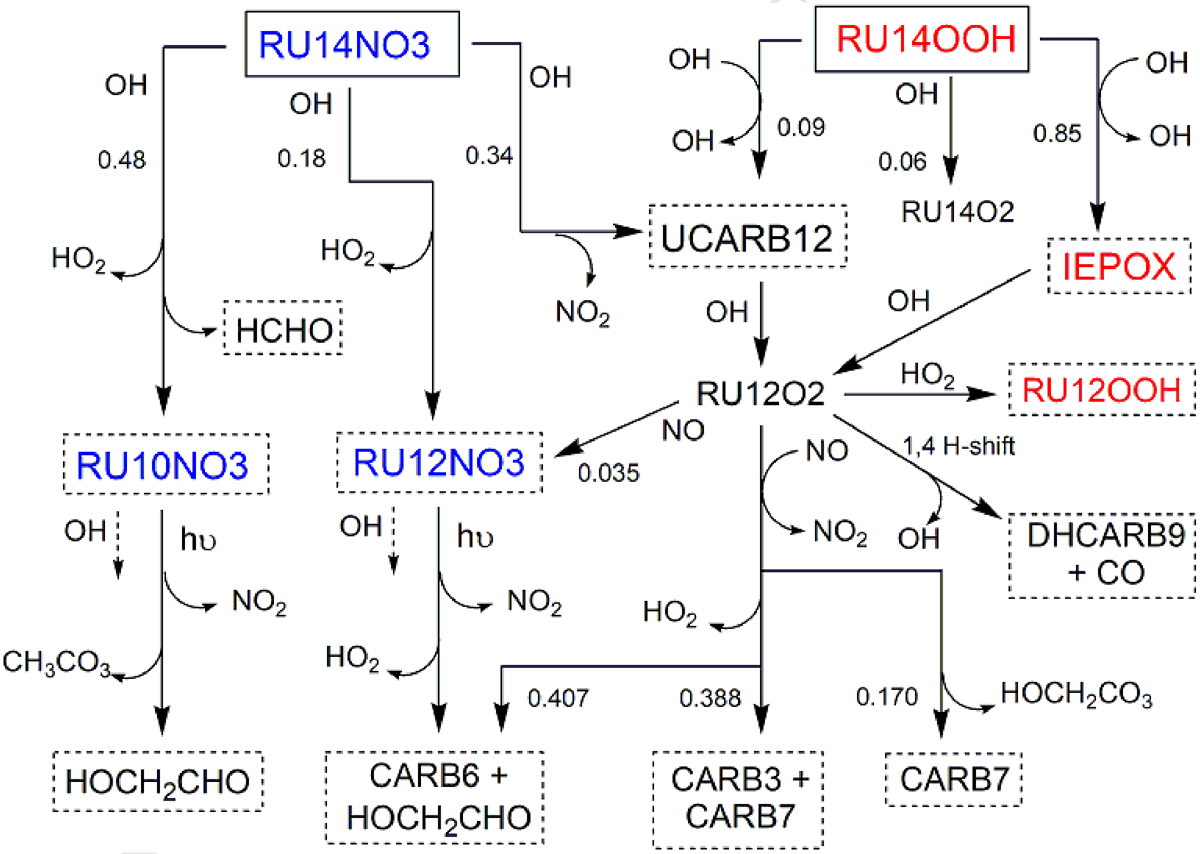

Figure 2: Schematic of the main features of the higher generation chemistry following oxidation of the lumped first-generation nitrate (RU14NO3) and hydroperoxide (RU14OOH), as represented in CRI v2.2; also incorporating the chemistry of the multi-generation product, UCARB12. Closed-shell organic products are shown in boxes. Species containing nitrate groups are shown in blue, and species containing hydroperoxide or epoxide groups are shown in red. For clarity, the scheme omits some minor initiation reactions and the reactions of RU12O2 with NO_3 and the peroxy radical pool, although these are included in the mechanism. Further information on species class and identity is given in Table S3.

3.2 Updates to the higher-generation chemistry

The rate parameters applied to the further oxidation of the lumped first-generation products are generally weighted averages of those applied to the contributing species in MCM v3.3.1. These were based on the relative yields of the contributing species in the middle of the range of NO_x levels considered in the zero-dimensional boundary layer box model simulations (i.e. at ~ 0.5 ppb NO_x).

Selected features of the second- and higher-generation chemistry are illustrated in Figs. 1, 2 and S4. Figure 1 shows the main features of the chemistry following the rapid photolysis of the newly defined lumped δ-hydroperoxyaldehyde product, HPUCARB12. This generates HO_x radicals, and leads significantly (50 %) to a lumped hydroxyvinyl carbonyl product (HUCARB9), which also photolyses rapidly to generate additional HO_x. This chemistry therefore substantially enhances the HO_x regeneration and production that results from the preceding 1,6 H-shift reaction of RU14O2.

Figure 2 summarizes the main features of the chemistry of the lumped first-generation hydroxynitrate (RU14NO3) and hydroperoxide (RU14OOH), formed from the reactions of RU14O2 with NO and HO_2, respectively. RU14NO3 is removed predominantly by reaction with OH radicals, with a lifetime of about 9 hours (for $[OH] = 1 \times 10^6$ molecule cm^{-3}). This represents a reduction in reactivity of almost a factor of two compared with CRI v2.1, reflecting that the distribution of the component species under atmospheric conditions contains a smaller contribution of the reactive δ-hydroxynitrate isomers in MCM v3.3.1 than represented previously in MCM v3.1 (see discussion in Jenkin et al., 2015). As shown in Fig. 2, the reaction of RU14NO3 with OH leads either to HO_x propagation and formation of products that retain the nitrate group (RU12NO3 and RU10NO3); or release of NO_x (as NO_2) and formation of products not containing oxidized organic nitrogen, represented by UCARB12. The second-generation nitrates, RU12NO3 and RU10NO3, are mainly representative of nitro-oxy carbonyl species in MCM v3.3.1, which have been reported to photolyse rapidly (Müller et al., 2014). Photolysis is therefore the dominant removal process assigned to RU10NO3 and RU12NO3, such that NO_x is effectively exclusively regenerated at this oxidation step.

The lumped first-generation hydroperoxide, RU14OOH, is removed predominantly by reaction with OH radicals, with a lifetime of about 4 hours. This mainly results in the OH-neutral conversion to a lumped epoxydiol product (IEPOX), consistent with the observations of Paulot et al. (2009) and Bates et al. (2014). The further oxidation of IEPOX is dominated by reaction with OH radicals, with a lifetime of about a day. This forms the lumped peroxy radical, RU12O2, which represents a set of unsaturated peroxy radicals containing hydroxyl and carbonyl groups. This is consistent with the major routes applied in MCM v3.3.1, which are based on the mechanism presented by Bates et al. (2014).

The major first generation products under the majority of atmospheric conditions are UCARB10 and formaldehyde, HCHO (see Fig. 1). UCARB10 is an unsaturated carbonyl species, which represents both methyl vinyl ketone (MVK) and methacrolein (MACR). The degradation of UCARB10 therefore incorporates the main features of the MVK and MACR chemistry as represented in MCM v3.3.1 with weighted average kinetic parameters and product ratios (see Fig. S4). Although much of this chemistry is unchanged from CRI v2.1, a 1,4 H-shift isomerization reaction is now incorporated for one of the product peroxy radicals, RU10AO2 (consistent with the study of Crounse et al., 2012), and the further OH-initiated oxidation of the second-generation product, methacryloyl peroxy nitrate (MPAN), now partially generates hydroxymethyl-methyl-α-lactone (HMML) in conjunction with release of NO_3 radicals. This represents the collective formation of the isomeric products, HMML and methacrylic acid epoxide (MAE), in MCM v3.3.1, which was based on the results of Kjaergaard et al. (2012) and Lin et al. (2013). In practice, the assumption applied in CRI v2.2 is more consistent with the more recent study of Nguyen et al. (2015), who report negligible formation of MAE.

4 Boundary layer box modelling studies

4.1 MCM v3.3.1 reference simulations

The MCM v3.3.1 simulations carried out using the zero-dimensional boundary layer box model have been reported and discussed in detail previously by Jenkin et al. (2015). These are used as the reference benchmark against which to compare the performance of CRI v2.2 and other mechanistic variants in the present work.

Wennberg et al. (2018) have reviewed recent laboratory and theoretical studies relevant to tropospheric isoprene degradation, and have compiled a detailed mechanism describing the gas-phase oxidation of isoprene and its major products. This takes account of information reported since the release of MCM v3.3.1, in particular a number of recent studies from the Caltech group of Wennberg and co-workers (e.g. Teng et al., 2017). Although the two mechanisms contain many common features, there are inevitably some mechanistic and parameter differences resulting from consideration of the more recent work by Wennberg et al. (2018), and from differing interpretations of the previously reported information. A series of the more important differences have therefore been implemented sequentially into MCM v3.3.1, resulting in the mechanistic variants denoted CAL 1 to CAL 4 in Table 1. The performances of these variants are compared with that of MCM v3.3.1 in Figs. 3 – 5 (with additional information and an extended discussion provided in Sect. S2). These illustrate the simulated daytime-averaged levels of a number of key species formed during isoprene degradation, and their dependence on the level of NO_x. The changes implemented in the mechanistic variants generally have only relative minor effects on mechanistic performance, such that the performance of MCM v3.3.1 is considered to remain an acceptable benchmark for the CRI v2.2 evaluation reported below.

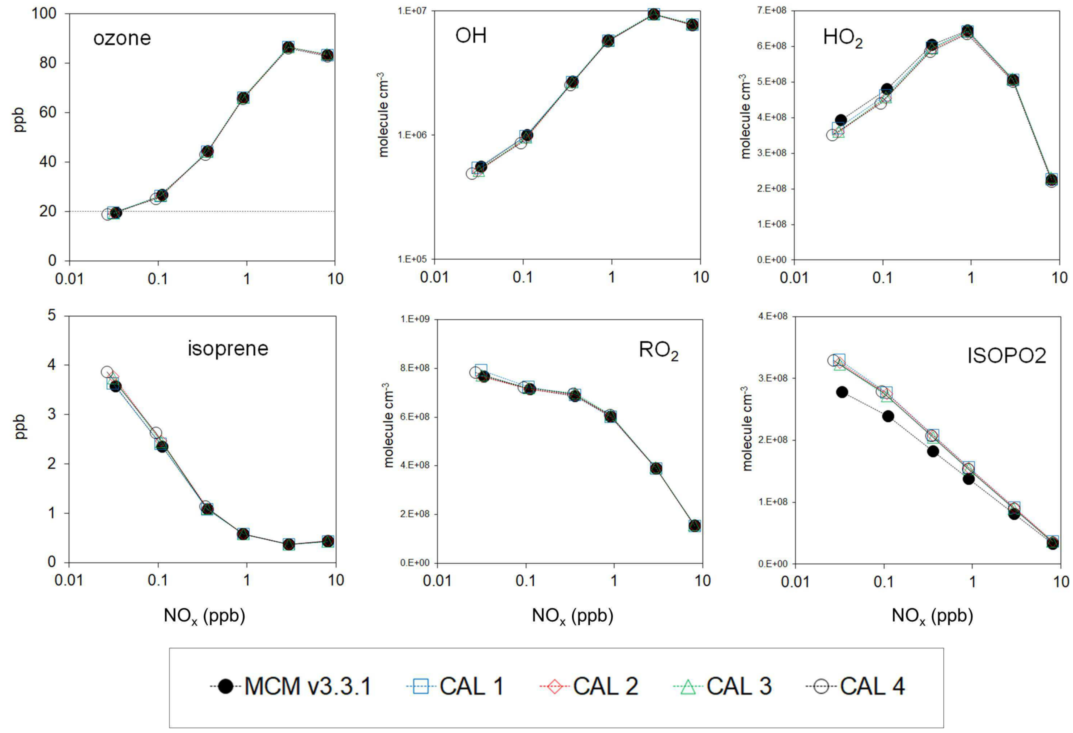

Figure 3: Comparison of performance of MCM v3.3.1 and the variants based on the Caltech scheme (Wennberg et al., 2018), showing the NO$_x$ dependence of the daylight-averaged mixing ratios or concentrations of O$_3$, isoprene, OH, HO$_2$, total organic peroxy radicals (denoted RO$_2$) and peroxy radicals formed from the first-generation OH-initiated chemistry (denoted ISOPO2). The broken line in the O$_3$ panel shows the background mixing ratio relative to which O$_3$ is either produced or destroyed (see text).

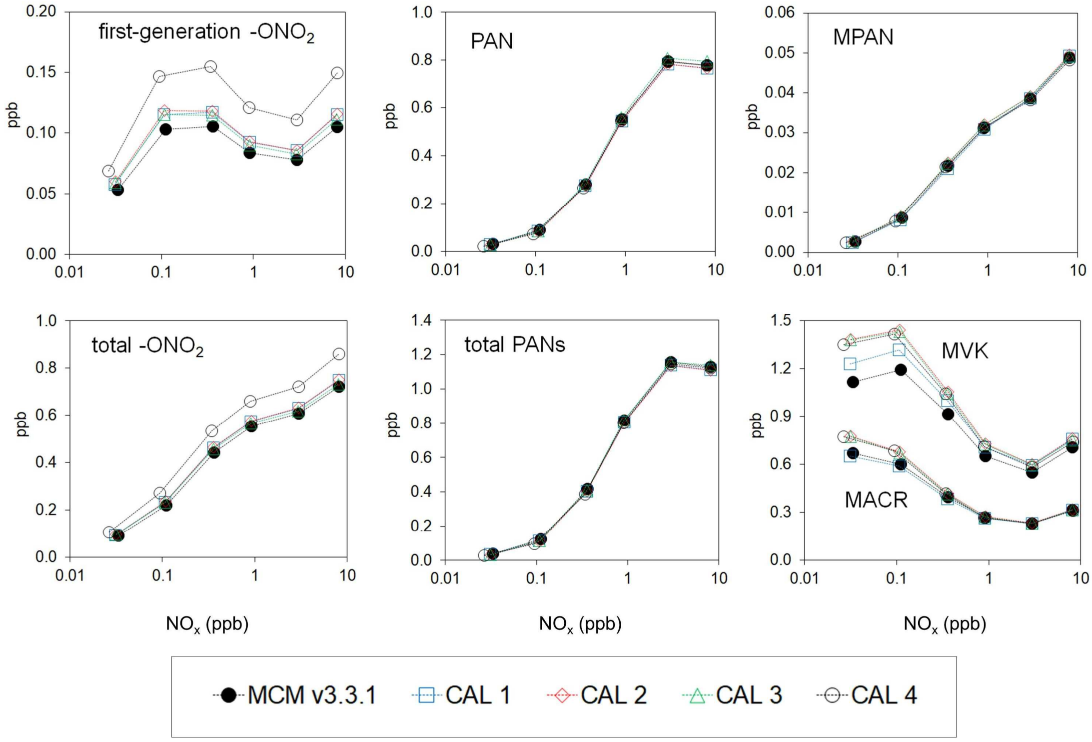

Figure 4: As Fig. 3 for the organic oxidized nitrogen reservoirs, nitrates (-ONO$_2$) and PANs; and methyl vinyl ketone (MVK) and methacrolein (MACR). The first-generation nitrates are specifically those formed from the reactions of NO with first-generation peroxy radicals (denoted “ISOPO2” in Fig. 3).

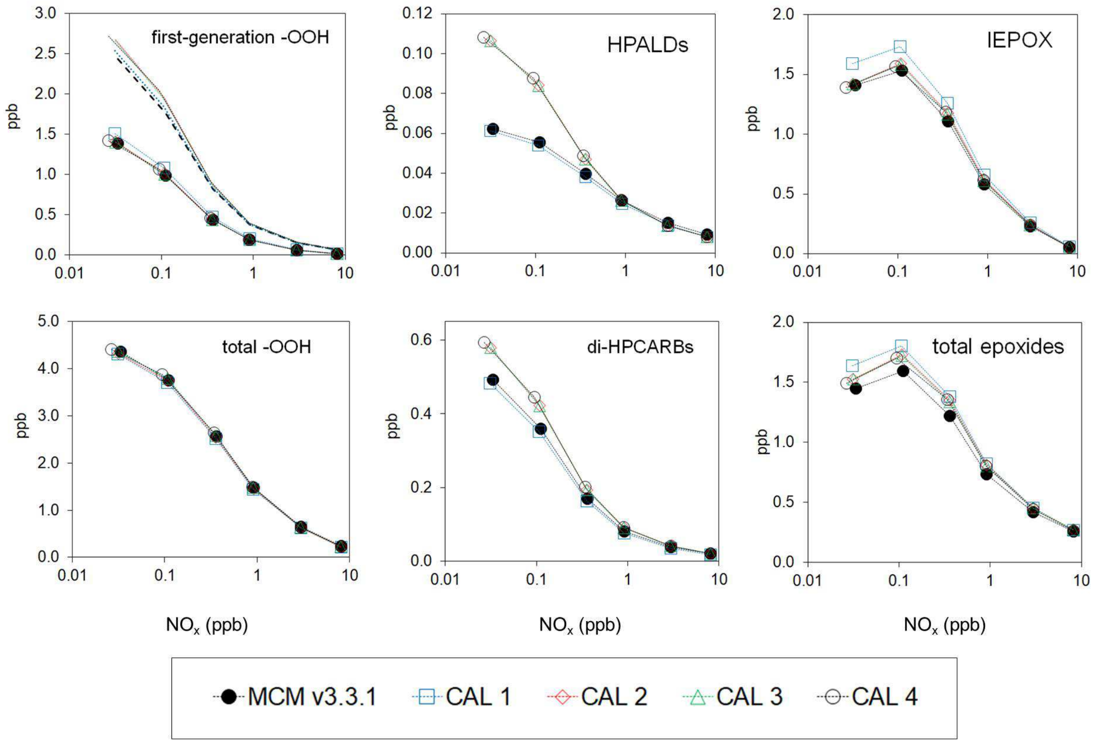

Figure 5: As Fig. 3 for selected hydroperoxides and epoxides. The first-generation hydroperoxides are specifically those formed from the reactions of HO_2 with first-generation peroxy radicals (denoted "ISOPO2" in Fig. 3). The additional lines in the "first-generation -OOH" panel shows the effect of including HPALDs and di-HPCARBs in the totals, with MCM v3.3.1 represented by the black heavy broken line and CAL 4 by the black light broken line.

Comparing the results obtained with CAL 4 (in which all the mechanistic changes listed in Table 1 were implemented) with the MCM v3.3.1 results reveals two notable differences in performance. First, the simulated collective levels of the unsaturated hydroperoxyaldehyde products (denoted HPALDs) are generally higher in the CAL 4 simulation (Fig. 5). Wennberg et al. (2018) represent partial formation of both β- and δ-hydroperoxyaldehydes from the chemistry following the 1,6 H shift isomerization reactions of the first-generation *Z*-δ-hydroxyperoxy radicals (tentatively based on the results of Teng et al., 2017), whereas only δ-hydroperoxyaldehydes are formed in MCM v3.3.1. The photolysis rate assigned to the β- isomers is an order of magnitude lower than that of the δ-isomers, owing to the aldehyde and unsaturated C=C groups being conjugated in the latter, but not in the former. This leads to the level of the β-hydroperoxyaldehydes being less supressed, resulting in higher total levels of HPALDs in the CAL2, CAL 3 and CAL4 simulations.

The second notable difference between the CAL 4 and MCM v3.3.1 simulations is an increasing suppression of the NO_x level towards the low end of the considered NO_x emission range in the CAL 4 results. This is because the fractional formation of hydroxynitrate products from the first-generation RO_2 + NO reactions recommended by Wennberg et al. (2018) is about 33 % higher (at 298 K and 760 Torr) than that applied in MCM v3.3.1. This higher sequestration of oxidized nitrogen is also apparent in the “first-generation $-ONO_2$” and “total $-ONO_2$” panels in Fig. 4. However, it is noted that this difference in the applied hydroxynitrate yields is well within the reported uncertainties (e.g. see discussion in Jenkin et al., 2015).

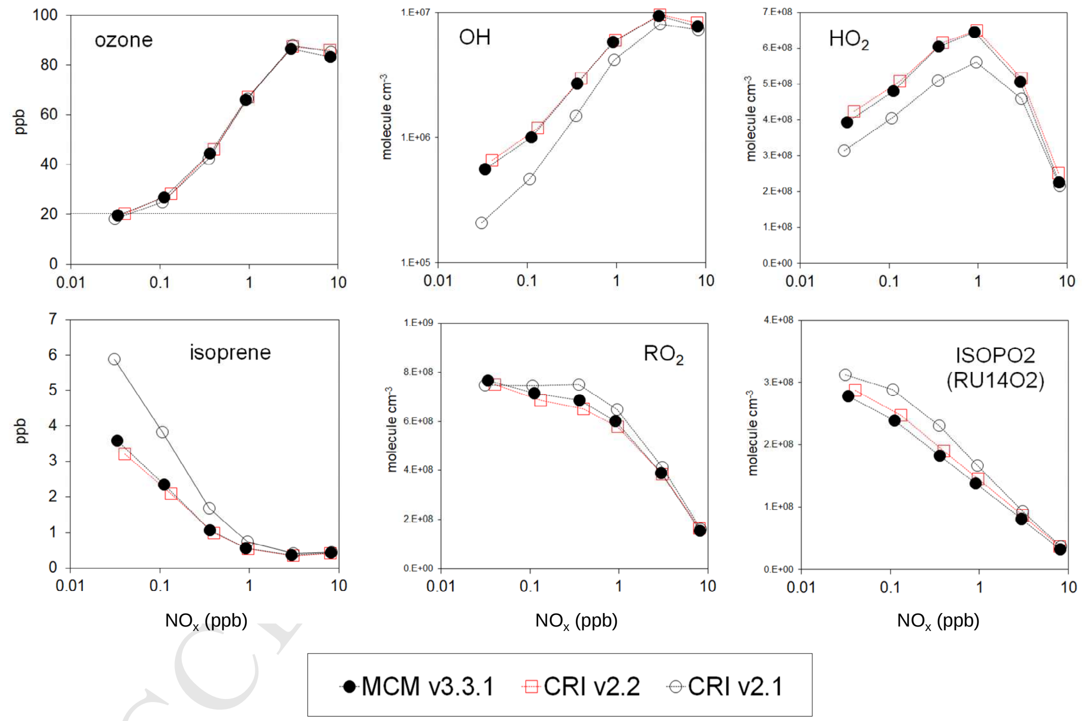

Figure 6: Comparison of performance of MCM v3.3.1, CRI v2.2 and CRI v2.1, showing the NO_x dependence of the daylight-averaged mixing ratios or concentrations of O_3, isoprene, OH, HO_2, total organic peroxy radicals (denoted RO_2) and peroxy radicals formed from the first-generation OH-initiated chemistry (denoted ISOPO2). The broken line in the O_3 panel shows the background mixing ratio relative to which O_3 is either produced or destroyed (see text). Where applicable, the name of the corresponding lumped CRI species is given in brackets (see also Table S3).

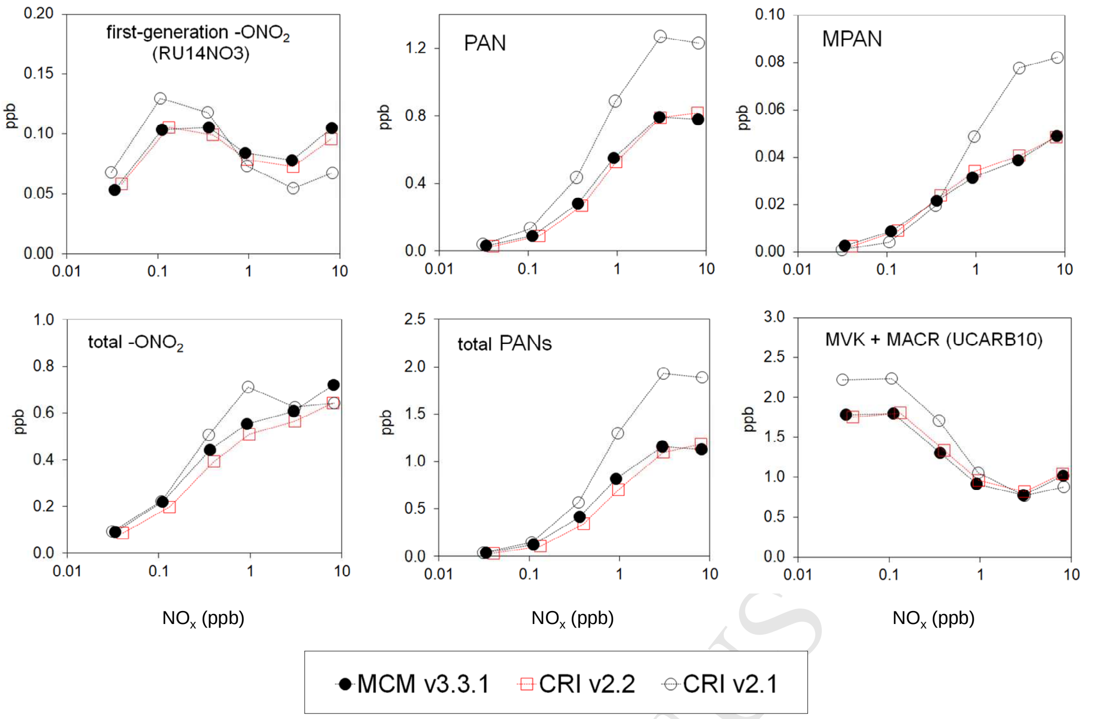

Figure 7: As Fig. 6 for the organic oxidized nitrogen reservoirs, nitrates (-ONO_2) and PANs, and the collective mixing ratio of MVK and MACR (in MCM v3.3.1) or UCARB10 (in CRI v2.2 and CRI v2.1). The first-generation nitrates are specifically those formed from the reactions of NO with first-generation peroxy radicals (denoted "ISOPO2" in Fig. 2). Where applicable, the name of the corresponding lumped CRI species is given in brackets (see also Table S3).

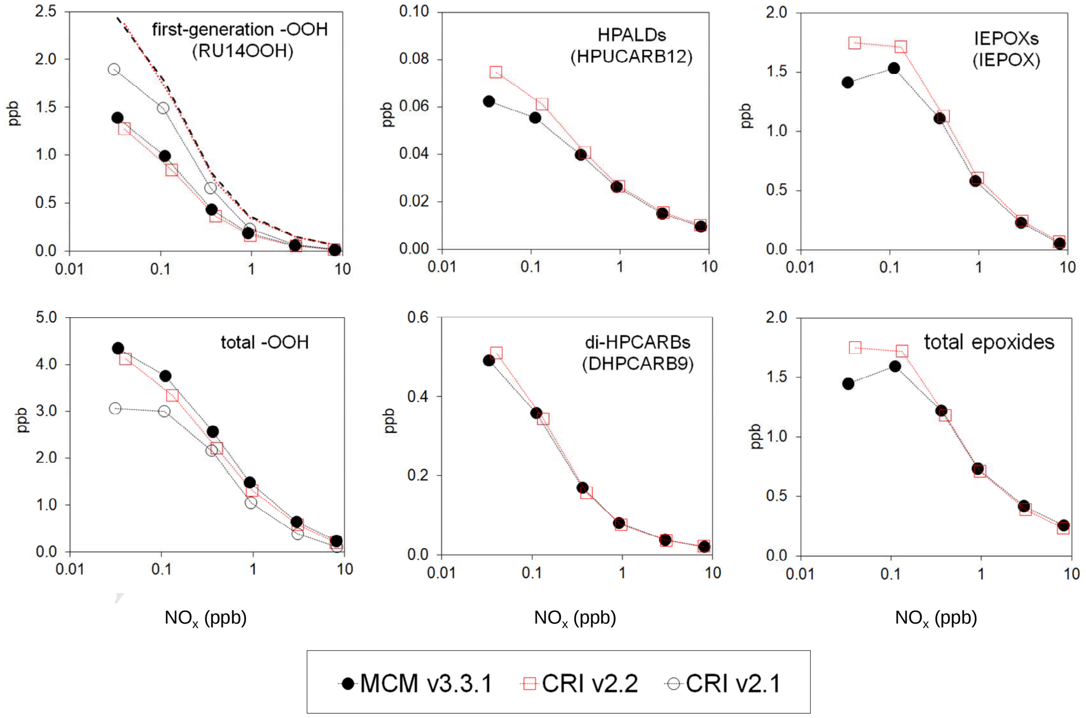

Figure 8: As Fig. 6 for selected hydroperoxides and epoxides. The first-generation hydroperoxides are specifically those formed from the reactions of HO_2 with first-generation peroxy radicals (denoted "ISOPO2" in Fig. 6). The additional lines in the "first-generation -OOH" panel shows the effect of including HPALDs and di-HPCARBs in the totals, with MCM v3.3.1 represented by the black heavy broken line and CRI v2.2 by the red broken line. Where applicable, the name of the corresponding lumped CRI species is given in brackets (see also Table S3).

4.2 CRI v2.2 simulations

The performances of CRI v2.2 and the preceding version, CRI v2.1, are compared with that of MCM v3.3.1 in Figs. 6 – 8. The results for the CRI v2.1 chemistry are comparable with those reported previously for MCM v3.1 (Jenkin et al., 2015), consistent with its performance being optimized to the earlier MCM version during development (Jenkin et al., 2008).

The results show that the changes implemented in CRI v2.2 bring its performance into generally good agreement with the current benchmark, MCM v3.3.1. Fig. 6 shows the impact of varying the NO_x input on the simulated concentrations of HO_x radicals, illustrating the well-documented suppression in the calculated OH concentrations as the NO_x levels decrease (e.g. Jenkin et al., 1993; 2015; Lelieveld et al., 2008). This results from the progressively decreasing efficiency of OH regeneration from the NO_x-catalysed free radical chemistry, and is particularly pronounced in the CRI v2.1 results, with the concentration of OH varying from a maximum of about 8×10^6 molecule cm^{-3} close to the high end of the NO_x range to about 2×10^5 molecule cm^{-3} at the low end of the range. The updates implemented in CRI v2.2 have a significant impact on OH radical regeneration at lower NO_x levels. The simulated OH concentrations are a factor of 3 greater at the low end of the NO_x range than those simulated with CRI v2.1, with this also suppressing the simulated isoprene mixing ratio. Fig. S5 confirms that the fluxes through the newly implemented OH regeneration routes are consistent with those simulated for the corresponding processes in MCM v3.3.1. These make a notable contribution at sub-ppb NO_x levels and collectively exceed that from the NO_x-catalysed free radical chemistry at NO_x levels below 100 ppt. Particularly important contributions are simulated to result from the chemistry initiated by the 1,6 H atom shift isomerization reaction of RU14O2 (including the subsequent rapid photolysis of HPUCARB12 and HUCARB9 and the 1,4 H shift reaction of DHPR12O2; see Sect. 3.1 and Fig. 1) and from the higher-generation 1,4 H atom shift isomerization reaction for RU10AO2 (see Sect. 3.2 and Fig. S4).

Fig. 7 shows that the updates in CRI v2.2 result in simulated abundances of oxidized organic nitrogen species that are in acceptable agreement with MCM v3.3.1. The simplified representation of the multi-generation chemistry in CRI v2.2 leads to total abundances of organic nitrates (i.e. species containing -ONO_2 groups) and PANs (i.e. species containing -C(O)$OONO_2$ groups) that are comparable to, although slightly lower than those simulated with MCM v3.3.1. This results in the NO_x levels being slightly less suppressed in the CRI v2.2 simulations, with this being most apparent towards the low end of the considered NO_x emission range. The simulations of hydroperoxides and epoxides in Fig. 8 also show that the updates in CRI v2.2 (described in Sect. 3) bring its performance into agreement with that of MCM v3.3.1, with those for UCARB10 and MPAN in Fig. 7 illustrating that the lumped representation of MVK and MACR chemistry (Sects. 3 and S1.2) provides a consistent description.

5 Global-scale modelling studies

Illustrative global scale simulations have been carried out using both the STOCHEM-CRI and EMEP MSC-W models. Implementation of the CRI v2.2 isoprene chemistry into STOCHEM-CRI was found to result in respective increases in the simulated global tropospheric OH and HO_2 burdens of 6.4 % and 0.8 % relative to those simulated using CRI v2. However, the distribution plots of OH concentration changes (Fig. 9) show that the inclusion of the new chemistry increased OH levels significantly over low NO_x and high isoprene emission regions, i.e. the terrestrial tropical forests (typically 15 – 30 %) and the boreal regions over Russia and Canada (typically 5 – 10 %). The increase in OH concentrations has in turn shortened the lifetime of isoprene, leading to a decrease in its tropospheric burden of 16.6 %. The increase in modelled OH concentrations over regions of the Amazon and Borneo results in levels that are more consistent with the high atmospheric oxidizing capacity measured and discussed by Lelieveld et al. (2008), Pugh et al. (2010) and Taraborrelli et al. (2012).

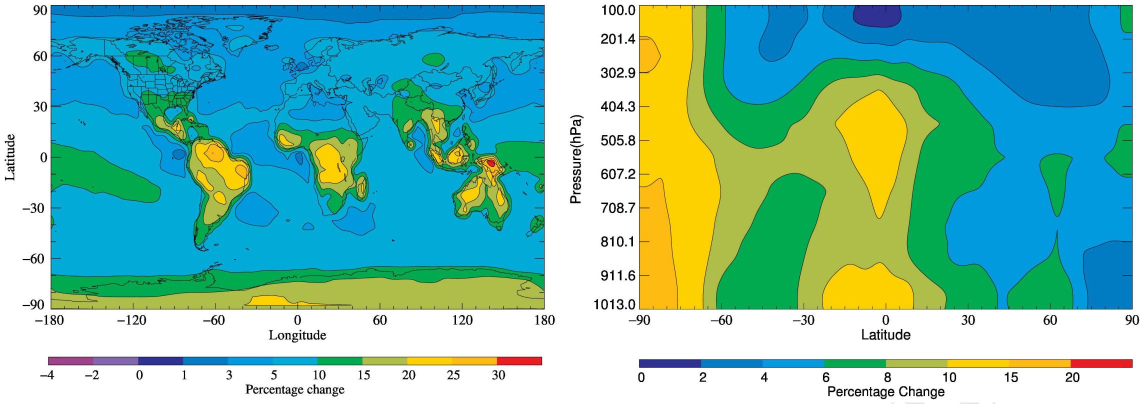

(a) (b)

Figure 9: The percentage changes of annual (a) surface [OH], (b) zonal [OH], simulated by STOCHEM-CRI following implementation of the CRI v2.2 isoprene chemistry. Simulations were carried out for 1998 and the results are mapped onto a Eulerian grid of dimensions 5° × 5° with nine equally vertically spaced pressure levels each ~100 hPa in thickness. Isoprene emissions were 501 Tg/yr from terrestrial vegetation and 1.9 Tg/yr from oceanic sources (see Sect. 2.2). Base case [OH] plots are provided in Sect. S3.

Implementation of the EMEP variant CRI v2.2 isoprene chemistry into EMEP MSC-W model similarly resulted in notable increases in surface OH and HO_2 concentrations (Fig. 10) relative to the CRI v2.1 isoprene scheme, these being > 10 % in most of the Americas, sub-Saharan Africa, Southern and Eastern Asia, and Oceania. Once again, particular OH enhancements (20 – 50 %) were simulated in the equatorial forested regions characterized by elevated isoprene emissions and low NO_x. The implementation of the updated isoprene chemistry in the two models therefore results in consistent impacts on the simulated terrestrial OH concentrations, given the differences in the applied meteorology, emissions and model resolution. However, the STOCHEM-CRI simulation also shows small enhancements in OH levels over the oceans which are not apparent in the EMEP MSC-W results. As will be discussed in more detail elsewhere, this mainly results from the recent inclusion of oceanic isoprene emissions in STOCHEM-CRI.

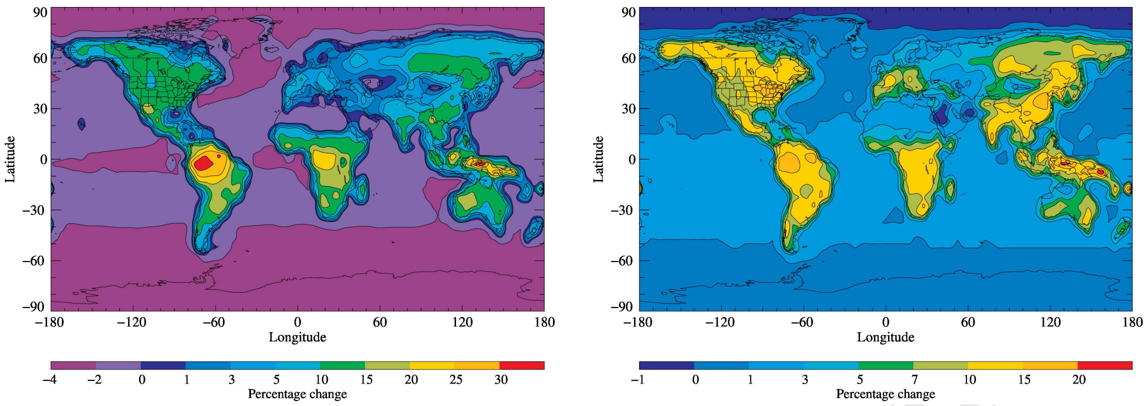

(a) (b)

Figure 10: The relative changes in annual (a) surface [OH] and (b) surface [HO_2], simulated by the EMEP MSC-W model following implementation of the EMEP variant CRI v2.2 isoprene chemistry. Simulations were carried out for 2010 with 1° × 1° grid resolution and are mapped at 5° × 5°. Isoprene emissions were 425 Tg/yr from terrestrial vegetation (see Sect. 2.2). Base case [OH] and [HO_2] maps are provided in Sect. S3.

---

6 Summary and conclusions

The chemistry of isoprene degradation in the Common Representative Intermediates (CRI) mechanism has been systematically revised and updated to reflect recent advances in understanding (as represented in MCM v3.3.1), with the revised chemistry being released as part of CRI v2.2. The complete isoprene degradation mechanism in CRI v2.2 is represented by 186 reactions of 56 species, which treat the chemistry initiated by reaction with OH, O_3 and NO_3. This is an order of magnitude reduction in size compared with MCM v3.3.1, in which isoprene degradation is represented by 1926 reactions of 602 species (Jenkin et al., 2015). A detailed overview of the updates has been provided, with reference to the reported kinetic and mechanistic information on which they are based. The revisions have impacts in a number of key areas, as illustrated by comparing the performance of the CRI v2.2 isoprene mechanism with that of the preceding version (CRI v2.1) over a range of relevant conditions in a box model of the tropical forested boundary layer. As a result, the revised representations of HO_x and NO_x recycling, and the production and removal of epoxide species, perform consistently with the corresponding processes in MCM v3.3.1. The revised isoprene chemistry has been shown to have significant impacts on simulated HO_x concentrations in global simulations using the STOCHEM-CRI and EMEP MSC-W chemistry-transport models.

The effects of recent advances in the understanding of isoprene degradation chemistry (as reviewed by Wennberg et al., 2018) have also been examined for a range of relevant conditions in the boundary layer box model, by implementing a series of the main mechanistic differences into the MCM v3.3.1 reference mechanism. Although there are some impacts on specific observables, the changes generally have only relative minor effects on overall mechanism performance. MCM v3.3.1 is therefore considered to remain an acceptable benchmark for evaluation of reduced mechanisms, and a practical platform for testing the impacts of newly discovered mechanistic information relevant to isoprene degradation.

Acknowledgements

The research presented is a contribution to the Swedish strategic research area ModElling the Regional and Global Earth system (MERGE), supported by the Swedish Formas grant 942-2015-1537 and Swedish Research Council (grant number 2014-5332). Additional support was provided by the UK Natural Environment Research Council (NERC) via grant NE/M013448/1 and the UK National Centre for Atmospheric Sciences (NCAS) Air Quality Science Programme. The EMEP modelling work was partially funded by EMEP under UNECE. Computer time for EMEP model runs was supported by the Research Council of Norway through the NOTUR project EMEP (NN2890K).

References

Andreae, M. O. and Crutzen, P. J.: Atmospheric aerosols: biogeochemical sources and role in atmospheric chemistry, Science, 276, 1052-1058, 1997.

Archibald, A. T., Cooke, M. C., Utembe, S. R., Shallcross, D. E., Derwent, R. G., and Jenkin, M. E.: Impacts of mechanistic changes on HO_x formation and recycling in the oxidation of isoprene, Atmos. Chem. Phys., 10, 8097-8118, doi:10.5194/acp-10-8097-2010, 2010a.

Archibald, A. T., Jenkin, M. E., and Shallcross, D. E.: An isoprene mechanism intercomparison, Atmos. Environ., 44, 5356-5364, doi:10.1016/j.atmosenv. 2009.09.016, 2010b.

Arneth, A., Monson, R. K., Schurgers, G., Niinemets, Ü., and Palmer, P. I.: Why are estimates of global terrestrial isoprene emissions so similar (and why is this not so for monoterpenes)?, Atmos. Chem. Phys., 8, 4605-4620, doi:10.5194/acp-8-4605-2008, 2008.

Arneth, A., Harrison, S. P., Zaehle, S., Tsigaridis, K., Menon, S., Bartlein, P. J., Feichter, J., Korhola, A., Kulmala, M., O'Donnell, D., Schurgers, G., Sorvari, S. and Vesala, T.: Terrestrial biogeochemical feedbacks in the climate system, Nature Geosci., 3, 525-532, 2010.

Arnold, S. R., Spracklen, D. V., Williams, J., Yassaa, N., Sciare, J., Bonsang, B., Gros, V., Peeken, I., Lewis, A. C., Alvain, S., and Moulin, C.: Evaluation of the global oceanic isoprene source and its impacts on marine organic carbon aerosol, Atmos. Chem. Phys., 9, 1253-1262, https://doi.org/10.5194/acp-9-1253-2009, 2009.

Bates, K. H., Crounse, J. D., St. Clair , J. M., Bennett, M. B., Nguyen, T. B., Seinfeld, J. H., Stoltz, B. M., and Wennberg, P. O.: Gas phase production and loss of isoprene epoxydiols, J. Phys. Chem. A, 118, 1237–1246, 2014.

Crounse, J. D., Knap, H. C., Ørnsø, K. B., Jørgensen, S., Paulot, F., Kjaergaard, H. G., and Wennberg, P. O.: Atmospheric fate of methacrolein. 1. Peroxy radical isomerization following addition of OH and O_2, J. Phys. Chem. A, 116, 5756–5762, 2012.

Derwent, R. G., Collins, W. J., Jenkin, M. E, Johnson, C. E and Stevenson, D. S.: The global distribution of secondary particulate matter in a 3-D Lagrangian chemistry transport model, J. Atmos. Chem., 44, 57-95, 2003.

Eerdekens, G., Ganzeveld, L., Vilà-Guerau de Arellano, J., Klüpfel, T., Sinha, V., Yassaa, N., Williams, J., Harder, H., Kubistin, D., Martinez, M., and Lelieveld, J.: Flux estimates of isoprene, methanol and acetone from airborne PTR-MS measurements over the tropical rainforest during the GABRIEL 2005 campaign, Atmos. Chem. Phys., 9, 4207–4227, 15, 2009.

Guenther, A. B., Jiang, X., Heald, C. L., Sakulyanontvittaya, T., Duhl, T., Emmons, L. K., and Wang, X.: The Model of Emissions of Gases and Aerosols from Nature version 2.1 (MEGAN2.1): an extended and updated framework for modeling biogenic emissions, Geosci. Model Dev., 5, 1471-1492, https://doi.org/10.5194/gmd-5-1471-2012, 2012.

Haagen-Smit, A. J., Fox, M. M.: Photochemical ozone formation with hydrocarbons and automobile exhaust., J. Air Pollut. Control Assoc., 4, 105-109, 1954.

Hallquist, M., Wenger, J. C., Baltensperger, U., Rudich, Y., Simpson, D., Claeys, M., Dommen, J., Donahue, N. M., George, C., Goldstein, A. H., Hamilton, J. F., Herrmann, H., Hoffmann, T., Iinuma, Y., Jang, M., Jenkin, M. E, Jimenez, J. L., Kiendler-Scharr, A., Maenhaut, W., McFiggans, G., Mentel, Th. F., Monod, A., Prévôt, A. S. H., Seinfeld, J. H., Surratt, J. D., Szmigielski, R., Wildt, J.: The formation, properties and impact of secondary organic aerosol: current and emerging issues, Atmos. Chem. Phys., 9, 5155-5236, 2009.

Jenkin, M. E. and Clemitshaw K.C.: Ozone and other secondary photochemical pollutants: chemical processes governing their formation in the planetary boundary layer, Atmos. Environ., 34, 2499-2527, 2000.

Jenkin, M. E., Murrells, T. P., Shalliker, S. J., and Hayman, G. D.: Kinetics and product study of the self-reactions of allyl and allyl peroxy radicals at 296 K, J. Chem. Soc. Faraday Trans., 89, 433-446, 1993.

Jenkin, M. E., Watson, L. A., Utembe, S. R., and Shallcross, D. E.: A Common Representative Intermediates (CRI) mechanism for VOC degradation. Part 1: Gas phase mechanism development, Atmos. Environ., 42(31), 7185-7195, 2008.

Jenkin, M. E., Young, J. C., and Rickard, A. R.: The MCM v3.3.1 degradation scheme for isoprene, Atmos. Chem. Phys., 15, 11433-11459, https://doi.org/10.5194/acp-15-11433-2015, 2015.

Khan, M. A. H., Jenkin, M. E., Foulds, A., Derwent, R. G., Percival, C. J. and Shallcross, D. E.: A modeling study of secondary organic aerosol formation from sesquiterpenes using the STOCHEM global chemistry and transport model, J. Geophys. Res. Atmos., 122, 4426–4439, doi:10.1002/2016JD026415, 2017.

Kjaergaard, H. G., Knap, H. C., Ornso, K. B., Jorgensen, S., Crounse, J. D., Paulot, F., and Wennberg, P. O.: Atmospheric fate of methacrolein. 2. Formation of lactone and implications for organic aerosol production, J. Phys. Chem. A, 116, 5763-5768, doi:10.1021/jp210853h, 2012.

Langner, J., Engardt, M., Baklanov, A., Christensen, J. H., Gauss, M., Geels, C., Hedegaard, G. B., Nuterman, R., Simpson, D., Soares, J., Sofiev, M., Wind, P., and Zakey, A.: A multi-model study of impacts of climate change on surface ozone in Europe, Atmos. Chem. Phys., 12, 10423-10440, doi:10.5194/acp-12-10423-2012, 2012.

Lelieveld, J., Butler, T. M., Crowley, J. N., Dillon, T. J., Fischer, H., Ganzeveld, L., Harder, H., Lawrence, M. G., Martinez, M., Taraborrelli, D., and Williams, J.: Atmospheric oxidation capacity sustained by a tropical forest, Nature, 452, 737–740, 2008.

Lin, Y.-H., Zhang, H., Pye, H. O., Zhang, Z., Marth, W. J., Park, S., Arashiro, M., Cui, T., Budisulistiorini, S. H., Sexton, K. G., Vizuete, W., Xie, Y., Luecken, D. J., Piletic, I. R., Edney, E. O., Bartolotti, L. J., Gold, A., and Surratt, S. D.: Epoxide as a precursor to secondary organic aerosol formation from isoprene photooxidation in the presence of nitrogen oxides, Environ. Sci. Technol., 110, 6718-6723, doi:10.1073/pnas.1221150110, 2013.

McFiggans, G., Mentel, T. F., Wildt, J., Pullinen, I., Kang, S., Kleist, E., Schmitt, S., Springer, M., Tillmann, R., Wu, C., Zhao, D., Hallquist, M., Faxon, C., Le Breton, M., Hallquist, Å. M., Simpson, D., Bergström, R., Jenkin, M. E., Ehn, M., Thornton, J. A., Alfarra, M. R., Bannan, T. J., Percival, C. J., Priestley, M., Topping, D. and Kiendler-Scharr, A.: Secondary organic aerosol reduced by mixture of atmospheric vapours, Nature, 565, 587-593, 2019.

Müller, J.-F., Peeters, J., and Stavrakou, T.: Fast photolysis of carbonyl nitrates from isoprene, Atmos. Chem. Phys., 14, 2497-2508, doi:10.5194/acp-14-2497-2014, 2014.

Nguyen, T. B., Bates, K. H., Crounse, J. D., Schwantes, R. H., Zhang, X., Kjaergaard, H. G., Surratt, J. D., Lin, P., Laskin, A., Seinfeld, J. H., and Wennberg, P. O.: Mechanism of the hydroxyl radical oxidation of methacryloyl peroxynitrate (MPAN) and its pathway toward secondary organic aerosol formation in the atmosphere, Phys. Chem. Chem. Phys., 17, 17914-17926, 2015.

Paulot, F., Crounse, J. D., Kjaergaard, H. G., Kürten, A., St. Clair, J. M., Seinfeld, J. H., and Wennberg, P. O.: Unexpected epoxide formation in the gas-phase photooxidation of isoprene, Science, 325, 730-733, 2009.

Peeters, J., Nguyen, T. L., and Vereecken, L.: HO_x radical regeneration in the oxidation of isoprene, Phys. Chem. Chem. Phys., 28, 5935-5939, 2009.

Peeters, J., Müller, J.-F., Stavrakou, T., and Nguyen, V. S.: Hydroxyl radical recycling in isoprene oxidation driven by hydrogen bonding and hydrogen tunneling: the upgraded LIM1 mechanism, J. Phys. Chem. A, 118, 8625-8643, 2014.

Peñuelas, J. and Staudt, M.: BVOCs and global change, Trends in Plant Science, 15(3), 133-144, doi:10.1016/j.tplants.2009.12.005, 2010.

Pugh, T. A. M., MacKenzie, A. R., Hewitt, C. N., Langford, B., Edwards, P. M., Furneaux, K. L., Heard, D. E., Hopkins, J. R., Jones, C. E., Karunaharan, A., Lee, J., Mills, G., Misztal, P., Moller, S., Monks, P. S. and Whalley, L. K.: Simulating atmospheric composition over a South-East Asian tropical rainforest: Performance of a chemistry box model, Atmos. Chem. Phys., 10, 279-298, 2010.

Saunders, S. M., Jenkin, M. E., Derwent, R. G. and Pilling, M. J.: Protocol for the development of the Master Chemical Mechanism, MCM v3 (Part A): tropospheric degradation of non-aromatic volatile organic compounds, Atmos. Chem. Phys., 3, 161-180, 2003.

Simpson, D., Winiwarter, W., Börjesson, G., Cinderby, S., Ferreiro, A., Guenther, A., Hewitt, C. N., Janson, R., Khalil, M. A. K., Owen, S., Pierce, T. E., Puxbaum, H., Shearer, M., Skiba, U., Steinbrecher, R., Tarrasón, L., and Öquist, M. G.: Inventorying emissions from nature in Europe, J. Geophys. Res., 104, 8113- 8152, 1999

Simpson, D., Benedictow, A., Berge, H., Bergström, R., Emberson, L. D., Fagerli, H., Flechard, C. R., Hayman, G. D., Gauss, M., Jonson, J. E., Jenkin, M. E., Nyíri, A., Richter, C., Semeena, V. S., Tsyro, S., Tuovinen, J.-P., Valdebenito, Á., and Wind, P.: The EMEP MSC-W chemical transport model – technical description, Atmos. Chem. Phys., 12, 7825-7865, https://doi.org/10.5194/acp-12-7825-2012, 2012.

Simpson, D., Wind, P., Bergström, R., Gauss, M., Tsyro, S. and Valdebenito, A.: Updates to the EMEP/MSC-W model, 2017-2018, in Transboundary particulate matter, photo-oxidants, acidifying and eutrophying components. Status Report 1/2018, The Norwegian Meteorological Institute, Oslo, Norway, www.emep.int, 109-116, 2018.

Simpson, D., Arneth, A., Mills, G., Solberg, S. and Uddling, J.: Ozone - the persistent menace; interactions with the N cycle and climate change, Curr. Opin. Env. Sust., 9-10, 9-19, 2014.

Stadtler, S., Simpson, D., Schröder, S., Taraborrelli, D., Bott, A. and Schultz, M: Ozone impacts of gas-aerosol uptake in global chemistry-transport models, Atmos. Chem. Phys., 18, 3147-3171, 2018.

Taraborrelli, D., Lawrence, M. G., Crowley, J. N., Dillon, T. J., Gromov, S., Groß, C. B. M., Vereecken, L. and Lelieveld, J.: Hydroxyl radical buffered by isoprene oxidation over tropical forests, Nature Geoscience, 5, 190-193, 2012.

Teng, A. P., Crounse, J. D. and Wennberg, P. O. Isoprene peroxy radical dynamics. J. Am. Chem. Soc., 139, 5367-5377, 2017.

Utembe, S. R., Cooke, M. C., Archibald, A. T., Jenkin, M. E., Derwent, R. G., Shallcross, D.E.: Using a reduced Common Representative Intermediates (CRIv2-R5) mechanism to simulate tropospheric ozone in a 3-D Lagrangian chemistry transport model, Atmos. Environ. 44, 1609-1622, 2010.

Warneke, C., de Gouw, J. A., Del Negro, L., Brioude, J., McKeen, S., Stark, H., Kuster, W. C., Goldan, P. D., Trainer, M., Fehsenfeld, F. C., Wiedinmyer, C., Guenther, A. B., Hansel, A., Wisthaler, A., Atlas, E., Holloway, J. S., Ryerson, T. B., Peischl, J., Huey, L. G. and Hanks, A. T. C.: Biogenic emission measurement and inventories determination of biogenic emissions in the eastern United States and Texas and comparison with biogenic emission inventories, J. Geophys. Res., 115, D00F18, doi:10.1029/2009JD012445.

Watson, L. A., Shallcross, D. E., Utembe, S. R., and Jenkin, M. E.: A Common Representative Intermediates (CRI) mechanism for VOC degradation. Part 2: Gas phase mechanism reduction, Atmos. Environ., 42(31), 7196-7204, 2008.

Wennberg, P. O., Bates, K. H., Crounse, J. D., Dodson, L. G., McVay, R. C., Mertens, L. A., Nguyen, T. B., Praske, E., Schwantes, R. H., Smarte, M. D., St Clair, J. M., Teng, A. P., Zhang, X. and Seinfeld, J. H.: Gas-phase reactions of isoprene and its major oxidation products, Chem. Rev., 118 (7), 3337-3390, 2018.

Went, F. W.: Blue hazes in the atmosphere, Nature, 187, 641-645, 1960.

The CRI v2.2 reduced degradation scheme for isoprene

M. E. Jenkin [*], M. A. H. Khan, D. E. Shallcross, R. Bergström, D. Simpson, K. L. C. Murphy and A. R. Rickard

Highlights

- Isoprene chemistry in a reduced (lumped chemistry) scheme is updated.
- Detailed MCM v3.3.1 isoprene chemistry is used as a reference benchmark.
- An order of magnitude reduction in species and reaction numbers is achieved.
- Performance of MCM v3.3.1 is tested in relation to recently reported information.
- Impacts of updates on global-scale [HO_x] are illustrated using two global models.

Declaration of interests

☒ The authors declare that they have no known competing financial interests or personal relationships that could have appeared to influence the work reported in this paper.

☐The authors declare the following financial interests/personal relationships which may be considered as potential competing interests: